Article

Cloning and functional analysis of *LtuPTOX*, a gene involved in carotenoid metabolism and orange band formation during tepal development in *Liriodendron tulipifera*

Ziyuan Hao[1], Yaxian Zong[1], Huanhuan Liu[1], Zhonghua Tu[1] and Huogen Li[1,2]*

[1] Key Laboratory of Forest Genetics & Biotechnology of Ministry of Education, Co-Innovation Center for Sustainable Forestry in Southern China, Nanjing Forestry University, Nanjing 210037, China; lxhzy1992@163.com (Z.H.); 1165269833@qq.com (Y.Z.); lhh91@foxmail.com (H.L.); zhonghuatu@njfu.edu.cn (Z.T.)

[2] College of Forestry, Nanjing Forestry University, Nanjing 210037, China

* Correspondence: hgli@njfu.edu.cn, Longpan Road, Xuanwu District, Nanjing, 210037, China

Abstract: Flower color and color patterns are important traits for ornamental species; for this reason, a comprehensive understanding of the genetic mechanisms underlying these characters is extremely significant for plant breeders. The tulip tree (*Liriodendron tulipifera* Linn.) is well known for its flowers, odd leaves and tree form. However, the genetic mechanism underlying its flower color remains unknown. In this study, a putative *LtuPTOX* gene was identified based on multiple databases of differential transcript expression at various developmental stages and the complete genome sequence of *Liriodendron*. Then, the full-length cDNA of *LtuPTOX* was derived from tepals and leaves using RACE approaches. Furthermore, the gene structure and a phylogenetic analysis of PTOX as well as AOXs, highly similar homologs in the AOX family, were used to distinguish between the two subfamilies of genes. In addition, transient transformation and qPCR methods were used to determine the subcellular localization and tissue expression pattern of the *LtuPTOX* gene. Moreover, the expression of *LtuPTOX* as well as pigment contents was investigated to illustrate the function of this gene during the formation of orange bands on petals. The results showed that the LtuPTOX gene encodes a 358-aa protein that contains a complete AOX domain (PF01768.17). Accordingly, *Liriodendron* PTOX and AOX genes were identified as only paralogs since they were rather similar in the sequence. LtuPTOX showed chloroplast localization, and expressed in the colored organs such as petals and leaves. In addition, increasing pattern of *LtuPTOX* transcripts lead to carotenoids accumulation on the orange-band in the development period of flower bud. Taken together, our results provide that *LtuPTOX* is involved in petal carotenoid metabolism and orange band formation in *L. tulipifera*. Meanwhile, the identification of this potentially involved gene will lay a foundation for further uncovering the mechanism of flower color formation in *L. tulipifera*.

Keywords: *L. tulipifera*, tepal, carotenoid biosynthesis, LtuPTOX, functional analysis

1. Introduction

Flower color is an important trait for ornamental species, as brightly colored flowers are more attractive to people. Additionally, color patterns and color spots play an essential role in attracting pollinators to insect-pollinated flowers, helping to improve the fitness of seeds and gene flow within species [1-3]. The response of pollinators to flower color is closely related to plant development and vigor [4]. Pigments in the petals have been extensively studied in many species [5,6], whereas the most important pigments in flowers are flavonoids, carotenoids and alkaloids[7].

Even many studies have focused on the formation of petal color in plants. In particular, the synthesis and degradation of anthocyanins have been illustrated during the past few years [7], yet the genetic mechanism of carotenoid metabolism remains unclear. One of the reasons for this ambiguity is that carotenoids are a subgroup of isoprenoid compounds that contain over 1158 isoforms, based on current knowledge [8]. Moreover, the genetic regulatory and metabolic pathways of carotenoids are not unique to C40 and other carotenoid categories. Nevertheless, the precursor for the synthesis of almost all carotenoids is isopentenyl diphosphate, an organic substance containing five carbon atoms [9,10]. Multistage catalysis involves a set of catalytic enzymes (including geranylgeranyl pyrophosphate (GGPP) synthase, phytoene synthase, phytoene desaturase (PDS), zeta-carotene desaturase (ZDS) and carotenoid isomerase (CRTISO), among others; see Fig. 1), but the precursors are ultimately converted to carotenes [9]. In addition, some co-factors such as phytochromes [11,12], electron mediators [13,14] and transcription factors [15] also participated in the synthesis of carotenoids.

Plastid terminal oxidase (PTOX) is a terminal oxidase involved in chlororespiration. The discovery of this gene took more than half a century. Diner and Mauzerall first revealed the positive feedback of oxygen in the photooxidation system almost fifty years ago [16]. Interestingly, this discovery indicated that there is a novel oxygen-dependent electron transport chain (ETC) in chloroplasts. Subsequently, in the 1980s, Bennoun proved that a photorespiration chain, which was similar to the respiratory ETC in mitochondria, also existed in the chloroplasts in plants [17]. In 1999, the *immutans* mutant of *Arabidopsis thaliana* brought attention to the PTOX gene [18,19]. Green and white stripes on the leaves of *immutans* confused researchers because they were not caused by the loss of enzymes in the chlorophyll synthesis pathway; the white sectors contained few carotenoids but accumulated phytoene [20]. The same pattern was also observed in the *ghost* mutant of tomato, with faded fruits, and further studies revealed that this abnormal phenotype was caused by the loss of PTOX gene function. In contrast to other enzymes in the carotenoid metabolic pathway, PTOX did not directly accelerate the conversion of intermediate products but accepted the electrons from PDS and ZDS and then delivered them as soon as possible (Fig. 1) [21]. Importantly, the absence of PTOX combined with the *IMMUTANS* and *GHOST* mutations almost impeded carotenoid accumulation. Hence, PTOX is considered an indispensable cofactor in the synthesis of carotenoids.

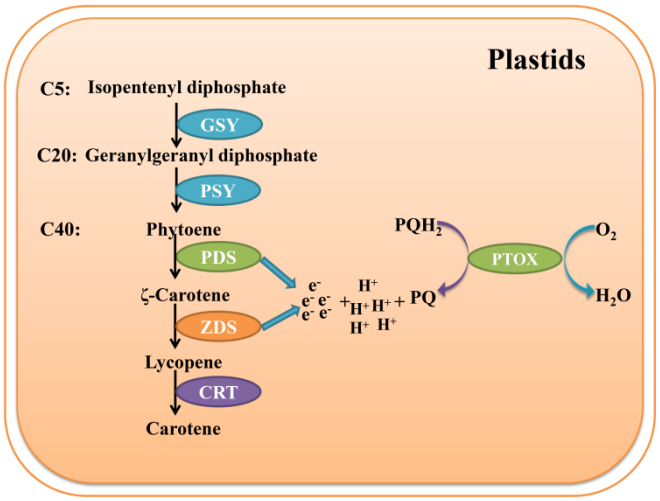

Fig. 1 PTOX participates in the process of carotenoid metabolism in plant plastids [9,14,21].

Liriodendron tulipifera originated in North America and was introduced to China decades ago to improve the adaptability and wood yield of *Liriodendron chinense*, a related species native to southern China. *L. tulipifera* is also well known as an ornamental tree species due to its odd leaf shape, brightly colored flowers and graceful tree form. Moreover, the tulip-like color and shape of the flowers give *L. tulipifera* another name: “tulip tree”. As a result, *Liriodendron* is often used for courtyard greening and street embellishment. In recent years, studies of *L. tulipifera* have focused on its origin and evolution [22,23], the development of its flowers and nectaries [24] and its interspecific breeding,

among other topics. Accordingly, attracted to the color and color patterns on the petals, specifically the orange band lying in the nectary area, Demuth also demonstrated that the main pigments in this area of *L. tulipifera* were carotenoids [25]. Even though the orange band is essential for aesthetic purposes and facilitating pollination, the genetic mechanism underlying the formation of this band remains unclear.

Inspired by previous research, we screened the candidate carotenoid synthesis gene *LtuPTOX* based on multiple databases. Moreover, the full-size cDNA of *LtuPTOX* was derived from *L. tulipifera* by rapid amplification of cDNA ends (RACE) approaches, and a subcellular localization assay and development-specific expression pattern analysis were carried out. Overall, this study revealed that the *LtuPTOX* gene participates in the synthesis of carotenoids and the development of the orange band on petals, which will be beneficial for characterizing the mechanism of flower color formation in *L. tulipifera*.

2. Materials and Methods

2.1. Plant materials

In early summer 2016, several tissues and organs, including leaves, flower buds, petals, stamens, pistils, leaf buds, flower buds and young stems, were removed from a living adult plant of *L. tulipifera* (seeds originating from South Carolina, USA), immediately frozen in liquid nitrogen, brought back to the laboratory and stored at -80 °C. Petals and leaves were used for gene isolation, and all the other tissues and organs were used to investigate the tissue-specific expression patterns of *LtuPTOX*. Petals at different developmental stages were obtained during the flowering period (from April to May 2017). All the *Liriodendron* trees were planted in Xiashu Forest Farm, which is attached to Nanjing Forestry University, Jiangsu Province, China. The *Nicotiana benthamiana* material used for the subcellular localization assay was obtained from the Key Laboratory of Forest Genetics and Biotechnology, Ministry of Education, Nanjing Forestry University. Trans T1 and GV3101 strains were used for gene cloning and transient expression, respectively.

Tobacco seeds were sterilized with 10% NaClO for 10 min and then sown in a nutrition matrix in an artificial illumination incubator under appropriate conditions (22 °C, with a 14-h light and 10-h dark photoperiod). Approximately 30 days after sowing, tobacco seedlings in the eight-leaf stage were used for transient transformation and subcellular localization analysis.

2.2. Identification and isolation of the full-length LcPTOX *gene in* L. tulipifera

Limited by the incomplete annotations of the Liriodendron genome database, we sought *LtuPTOX*-homologous genes by using a multidatabase approach, including the classical expressed sequence tag (EST) database [26] of *L. tulipifera* (AAGP, http://jlmwiki.plantbio.uga.edu/aagp/), and a local RNA-seq database of distinct flowering stages obtained by Illumina NovaSeq (presented in another article under review). Because the EST fragments were short and incomplete, we mapped all the *LtuPTOX* fragments obtained from the EST database to the local RNA-seq differentially expressed gene (DEG) database and the recently released genome database of *L. chinense* [23]. Redundant sequences were removed, differential expression at distinct stages was considered, and a putative *LtuPTOX* gene was obtained for further study. To obtain the full sequence of *LtuPTOX*, we further developed a RACE assay to drive the target sequence. Gene-specific primers (see the Appendix A) were used to isolate 5′ and 3′ untranslated regions. Sequences of intermediate and 5′ and 3′ untranslated regions were finally assembled by DNAstar software.

2.3. Structural and functional identification of LtuPTOX by bioinformatic approaches

To preliminary understand the function and properties of LtuPTOX, a series of software and approaches were used for analysis. The LtuPTOX protein sequence was obtained by submitting the full-length cDNA of the LtuPTOX gene to an online tool (https://www.ncbi.nlm.nih.gov/orffinder/) for open reading frame (ORF) prediction. The physicochemical properties of the LtuPTOX protein were analyzed using ExPASy ProtParam online software (https://web.expasy.org/protparam/).

Moreover, the conserved domain of the LtuPTOX protein was determined by Pfam (http://pfam.xfam.org/), and tertiary structure prediction was performed with I-TISSER software [27]. Location and structural information of the LtuPTOX gene was further obtained by genome-wide identification. Accordingly, the differences in gene structure between AOX and PTOX were assessed using GSDS 2.0 software [28], since the genes have been considered homologous genes over the past years. Additionally, sequences were aligned with those from other species and visualized by ESPrint 3.0 software [29]. We further performed a standard phylogenetic analysis, using MAFFT software [30,31] for multiple sequence alignment and Gblocks 0.91 software [32] for conserved domain selection. Finally, an optimal amino acid substitution model was selected using MEGA7 software, and with this optimum model, the phylogenetic relationships were demonstrated with a neighbor-joining (NJ) tree.

2.4. Transient expression and subcellular localization of the LtuPTOX *gene*

The pCAMBIA1302 vector was digested by NcoI and SpeI quick-cut enzymes (TAKARA), and then, we inserted the complete ORF sequence into the digested pCAMBIA1302 vector. Furthermore, the raw pCAMBIA1302 vector and the recombinant vector carrying the *35S:LcPTOX-GFP* gene were transferred into the GV3101 *Agrobacterium* strain. With the P19 helper vector, two expression stains were injected into the lower epidermis of tobacco leaves. After 2 ~ 3 days of incubation at 23 °C, the lower epidermis of infected tobacco leaves was removed carefully and placed on a glass slide, and then we observed the slices at distinct wavelengths using a laser confocal microscope (LSM710).

2.5. Expression pattern of the LtuPTOX *gene in various tissues/organs*

Eight tissues and organs, namely, mature leaves, flower buds, petals, stamens, pistils, leaf buds, flower buds and young stems, were removed from the *L. tulipifera* adult for RNA extraction and expression pattern determination. Quantitative PCR primers were designed according to the full-length cDNA sequence of the *LtuPTOX* gene (Appendix A), and the reactions were performed using SYBR Premix Ex Taq enzyme (RR420A, TAKARA) according to the instructions for the ABI Step-One Plus platform. The relative expression of genes was calculated and plotted with Microsoft Office 2010 and GraphPad 7.0 software.

2.6. Expression levels of the LtuPTOX *gene within the orange petal band at different stages*

Petals at various developmental stages, from S1 to S5, were used to determine the expression changes of the *LtuPTOX* gene. The five petal developmental stages are described in Fig. 5a: S1, female flower buds begin to enlarge, and the flower bud is as hard as a marble; S2, intermediate developmental stage of female flowers, when the flower buds begin to soften; S3, later enlargement phase of the flower bud, when the orange band of the petals appears yellow; S4, the flower buds are preparing to open, and the color of the orange band of the petals begins to deepen; and S5, the peak flowering period of Liriodendron flowers, when pollination and fertilization begin. Orange band tissue at five stages was used for RNA extraction and expression determination according to the manufacturer's instructions (RR036A and RR420A, TAKARA). The experiments were performed with the ABI Step-One Plus platform, and then we calculated expression with Microsoft Office software.

2.7. Quantification of chlorophyll and carotenoid contents in the orange petal band

We further removed the orange band region of Liriodendron petals at different stages for chlorophyll and carotenoid determination. In vitro tissues were pulverized in liquid nitrogen, and all the materials were standardized to 0.1 g. Then, 10 ml of extraction liquor (80% acetone and 20% absolute ethanol) was added to the centrifuge tube. After 2 days of extraction at 37 ℃ in dark conditions, when the materials were thoroughly faded, the mixed liquor was centrifuged at 12000 rpm. Afterwards, the supernatants were collected to determine pigment content. Moreover, we detected the absorbance value at multiple wavelengths (470 nm, 647 nm and 663 nm). Finally, the

chlorophyll and carotenoid contents were calculated according to the method of Arnon and Myeong J. K. [33,34]. The equation is provided as follows:

$$\text{ChlA (mg/g FW)} = [(12.7\times(A) - 2.69\times(B))/(D\times1000\times W)]\times V, \quad (1)$$

$$\text{ChlB (mg/g FW)} = [(22.9\times(B) - 4.68\times(A))/(D\times1000\times W)]\times V, \quad (2)$$

$$\text{Chl (mg/g FW)} = [(20.29\times(B) + 8.02\times(A))/(D\times1000\times W)]\times V, \quad (3)$$

$$\text{CxC (mg/g FW)} = [((1000\times(C) - 1.82\times(\text{ChlA}) - 85.02\ (\text{ChlB}))/198)/(D\times1000\times W)]\times V. \quad (4)$$

3. Results

3.1. Full length cDNA isolation of LtuPTOX *gene*

Six EST fragments annotated as PTOX or IMMUTANS (Table.1) were obtained from the *L. tulipifera* EST database [26] (AAGP, http://jlmwiki.plantbio.uga.edu/aagp). To generate the target sequence of the *LtuPTOX* gene and DEGs associated with petal development, alignments of the 6 fragments were performed with the DEG database at different developmental stages. By perfect alignments and the removal of redundant sequences, a unigene named Liriodend_newGene_31435 was ultimately obtained. We searched for the unigene in the genome-wide sequences of *L. chinense* and found that the Lchi07087 gene was extremely consistent with Liriodend_newGene_31435. Afterwards, a gene-specific primer was designed to isolate the full-length cDNA of LtuPTOX.

Intermediate and 5′ and 3′ untranslated regions were amplified in vitro under different conditions, and their lengths were 764 bp, 396 bp, and 468 bp, respectively (Appendix B). We further assembled the three fragments *in silico* using DNAstar software, and primers were assigned at both ends of the sequence for full-length isolation. Finally, we obtained the complete sequence of the *LtuPTOX* gene.

Table 1. Screening and identification of LtuPTOX from multiple *Liriodendron* database

AAGP gene NO.[1]	RNA-seq dataset	Gene ID[2]	Annotation
gnl|Liriodendron|b4_c3586 gnl|Liriodendron|b4_c15469 gnl|Liriodendron|b4_c23296 gnl|Liriodendron|b4_c24190 gnl|Liriodendron|b4_s124823 gnl|Liriodendron|b4_rep_c78233	Liriodend_newGene_31435	Lchi07087	PTOX/IMMUTANS

1, AAGP data base: http://jlmwiki.plantbio.uga.edu/aagp;
2, Genome Database: ftp://ftp.cngb.org/pub/CNSA/CNP0000295/CNS0044063/CNA0002404/.

3.2. In silico *analysis of the function and structure of* LtuPTOX *gene*

The full-length ORF of the LcPTOX gene is 1077 bp long and encodes a 358-amino acid (aa) protein (GenBank ID: MN368606). The molecular weight of LtuPTOX is approximately 41.3 kDa, and the theoretical isoelectric point is 5.98, which provides evidence for the faint acidity of the LtuPTOX protein. Multiple protein sequence alignments were performed in DNAMAN and ESPrint software, and the identity of PTOX was approximately 72.54%. The PTOX protein shared a conserved domain from 85 aa to 313 aa (PF01768.17) with AOX, and "ExxH" Di-iron coordination motifs, which were considered iron binding sites in many other studies [35], were found in this region (Fig. 2a). Subsequently, we compared the gene structure of *PTOX* with that of *AOX*, a paralog located in mitochondria based on *Liriodendron* genome sequences, as they were often mistakenly placed in the same category in previous studies. The *Liriodendron* AOX protein possesses four exons and three introns, and the PTOX gene possesses nine exons and eight introns. Moreover, the AOX

protein contains two " ExxH" motifs, both of which are located in the third exon. However, the two " ExxH" motifs are distributed in the fifth and ninth exons, respectively (Fig. 2b).

PTOXs of several other species, including six spermatophytes and two algae, were used for phylogenetic analysis (GenBank accessions: SlPTOX, NP 001234511.1; CaPTOX, AAG02288.1; CcPTOX, ABB70513.1; DcPTOX, AJE24555.1; GmPTOX, NP_001242139.2; LtuPTOX, MN368606; AtIMMUTANS, AJ004881; OsPTOX, AF085174; AtIMMUTANS, AJ004881; HlPTOX, ABF85789.1; CrPTOX, XP_001703466.1; LcAOX1a, MN187966; LcAOX1b, MN187968; and LcAOX2, MN187967). To correct the NJ tree, the LcAOXs were also included as an outgroup in this process. Three categories, namely, spermatophyte, alga and outgroup, are clearly displayed in Fig. 2c. Moreover, the genetic relationship between OsPTOX and LtuPTOX was closer than that between other pairs, according to the phylogenetic tree.

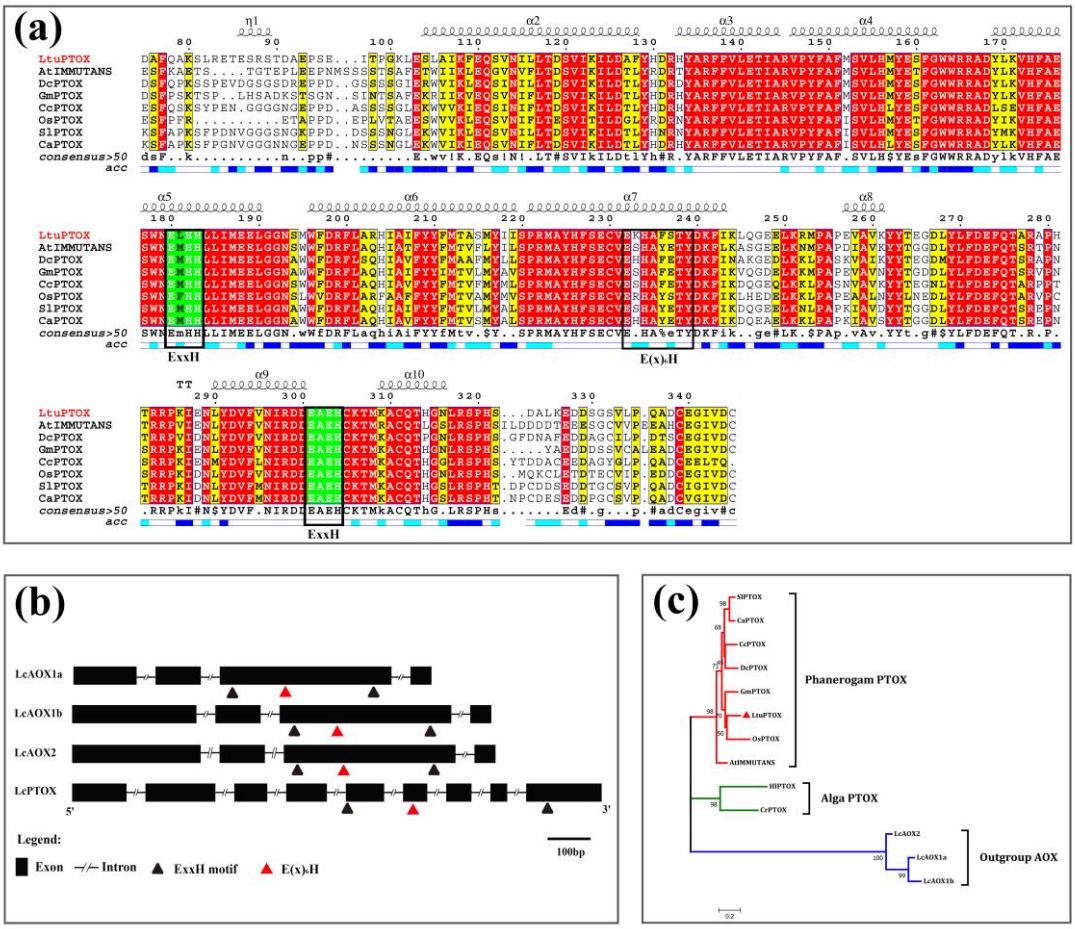

Fig. 2 Sequence alignment and phylogenetic analysis of LtuPTOX (a), Multiple sequence alignment of PTOXs, where the helixes on top of the lines are α-helixes, blue and white bars indicate the site accessibility of the protein (blue bars represent the amino acids that are accessible, cyan bars represent those with intermediate accessibility, and white bars indicate those that are not accessible . ExxH modules with a green background are the putative di-iron coordination motifs. (b), Gene structure comparison of *Liriodendron* PTOX and AOXs, where rectangles represent exons, lines represent introns, and triangles represent di-iron coordination motifs. (c), Phylogenetic analysis based on PTOXs and the *Liriodendron* AOXs.

3.3. Transient transformation and subcellular localization of LtuPTOX

Determining the subcellular localization of a protein is critical in establishing its function. By expressing a fusion gene of *LtuPTOX* and *eGFP* in epidermal cells using tobacco transient expression approaches, we successfully determined the subcellular localization of the LtuPTOX proteins. On the laser confocal microscope platform, green fluorescence of the tobacco cells in the control group, which carried *35S:eGFP* genes, displayed a global expression pattern. However, green signals in the

tobacco cells modified by the *35S:LtuPTOX-eGFP* gene showed the same location as chloroplasts in the lower epidermis (Fig. 3). Based on these results, the LtuPTOX protein might play a significant role in chloroplasts, which is consistent with the finding of its potential function as a protective factor for chlorophyll in many other studies [21,36-38]. However, in other cases, *PTOX* genes also play important roles in nonchlorophyllous tissues [39,40].

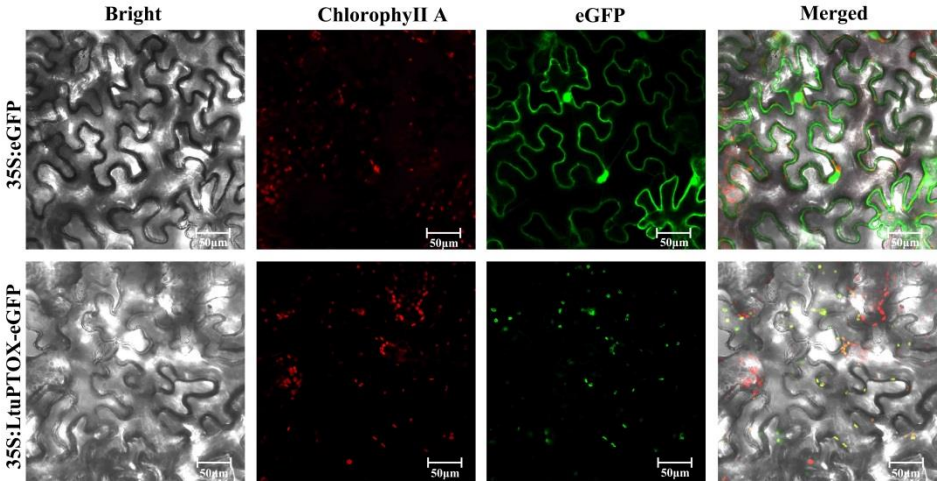

Fig. 3 Subcellular localization of LtuPTOX in tobacco leaves

3.4. Expression pattern of the LtuPTOX *gene in various tissues/organs*

In order to understand the expression pattern of the *LtuPTOX* gene in various tissues and organs, we used qRT-PCR to determine the relative expression of *LtuPTOX*. The qPCR results showed that petals possessed the highest abundance of transcripts, followed by calyxes and leaves (Fig. 4). The expression in these three tissues was far greater than that in the other tissues and organs in this assay, which suggested that tissues containing many pigments (e.g., chlorophyll and carotenoids) might also contain a large number of *LtuPTOX* transcripts. In many cases, PTOX acts as a safety valve in the photosynthetic system [41]; however, we detected very high enrichment in tissues in which green pigments gradually faded and even in nonchlorophyllous tissues, such as the petals. Hence, we inferred that *LtuPTOX* is more than just a safety valve for chlorophyll.

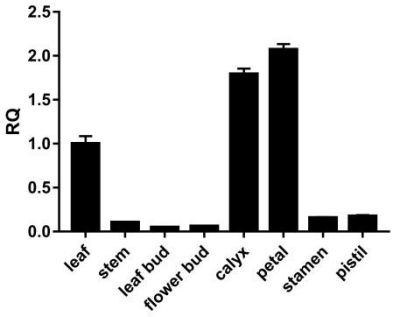

Fig. 4 Expression patterns of *LtuPTOX* in eight tissues/organs

3.5. LtuPTOX *involved in carotenoids metabolism and orange-band formation on the tepal*

To thoroughly investigate the relationship between *LtuPTOX* expression and flower color changes in *L. tulipifera*, orange petal band tissues at different developmental stages were used for RNA extraction and expression detection (Fig.5a). Although the orange band region on the petals did not initially appear to be green, the results of both quantitative and semiquantitative PCR demonstrated upward trends as the color of the petals deepened (Fig. 5b). In a previous study, discoloration of tomato fruits was shown to be caused by a loss-of-function mutation in the PTOX allele, and then the transformation of phytoene and ζ-carotene was blocked [19,42]. We further

quantified the chlorophyll and carotenoid contents in orange petal bands at different developmental stages. The chlorophyll content decreased gradually with petal development and reached zero in the later flower bud enlargement phase (S3). In striking contrast to chlorophyll, carotenoids accumulated rapidly beginning in the S3 period (Fig. 5c). The change in *LtuPTOX* expression was highly consistent with the carotenoid content accumulation, and the same pattern was also found in *Arabidopsis* seedlings [19] and tomato fruits [42]. In summary, LtuPTOX is a critical gene involved in the formation of orange bands on petals.

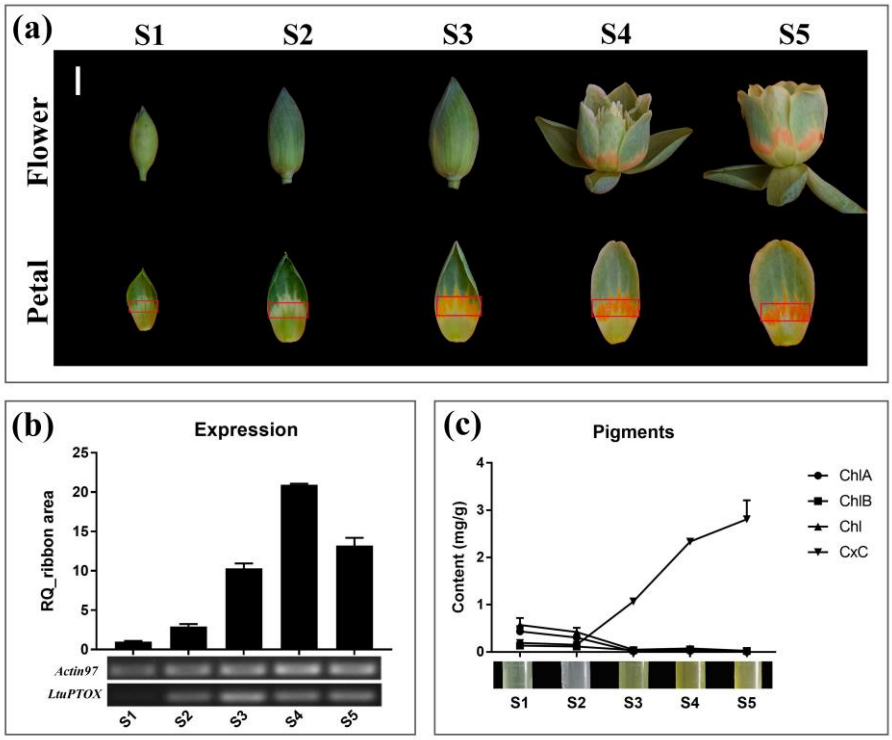

Fig. 5 Changes in pigment content and gene expression in the orange bands of Liriodendron petals during different developmental stages. (a), are the different developmental stages of the materials examined, the orange band marked by a red box on each of the petals was used for RNA extraction and pigment determination, and the bar is 1 cm; (b), Changes in the expression level of the LtuPTOX gene from S1 to S5. (c), Changes of the four pigments content in different developmental stages, including chlorophyllA (ChlA), chlorophyllB (ChlB), total chlorophyll (Chl), and Carotenoids (CxC).

4. Discussion

In this study, a putative *LtuPTOX* encoding a 358-aa protein was derived from *L. tulipifera* through multiple alignments and gene screening against the RNA-seq DEG database as well as the complete genome sequence of *L. chinense*. An AOX conserved domain from 85 aa to 313 aa was identified in the LtuPTOX protein sequence, which indicated its similarity to the PTOX and AOX gene sequences. *PTOX* genes are often compared with *AOX* genes, as they have similar sequences and share the same conserved domains. The results of evolutionary analysis showed that these genes were derived from the same ancestral gene [43,44]. Moreover, an active site, "E(x)6Y", detected by Nakamura was also found in the conserved domain in both subfamilies [45], as were two di-iron coordination motifs named "ExxH", although they were quite different in gene structure and location [9]. This structural consistency might lead to a strong similarity in function in many cases, such as the functional redundancy of the two subfamily proteins of *A. thaliana* detected in chloroplasts [46]. In contrast to the respiratory ETC in mitochondria, the photorespiration ETC carries a distant terminal oxidase, which is able to transfer electrons from NADH/NADPH to plastoquinone (PQ) [47].

Based on previous studies, PTOX is a terminal oxidase involved in chlororespiration that regulates the redox state of the PQ pool [48] by transferring excess electrons to O2 in order to maintain the relative redox balance in the photosynthetic ETC. In this study, chloroplast subcellular localization of LtuPTOX was observed in tobacco leaves, which was consistent with the safety valve function of this gene in photorespiration and stress responses [14,37,49]. The same gene participates in the synthesis of carotenoids in *A. thaliana* and *Solanum lycopersicum* [19,39], even though tomato fruits do not contain chloroplasts. In addition, the dual role of PTOX was further characterized in different plastids of these two model plants [9,13]. Besides, the high expression level of LtuPTOX in colored organs and tissues provided an additional line of evidence.

As a common sense, plastids are of great difference to plant cells depending on the pigments or other metabolites they contained in higher plants. In addition to chloroplasts, other well-known plastids, such as colored bodies, yellow bodies, white bodies, amyloids, protein bodies, and oil bodies, are found in different vegetables. However, these various types of plastids are able to rapidly interconvert under some special conditions [50]. In this manner, we inferred that LtuPTOX might be a multifunctional enzyme in *L. tulipifera*.

Finally, we illustrated the fact that the expression of *LtuPTOX* increased in the orange-band region during the period of tepal development. Meanwhile, we also demonstrated the complete synchronicity of gene expression and carotenoid accumulation during this period, especially the abrupt increase that occurred from S2 to S3. Consistent with our results, novel pathways of electron transport mediated by AtPTOX were recently found in etioplasts of *Arabidopsis* [51]. Kambakam found that AtPTOX coupling with PGR5 and the NDH complex caused electron transfer from PDS and ZDS to PQH2 in the carotenoid biosynthesis pathway under dark conditions. Despite the absence of virus-induced gene silencing (VIGS) methods in *Liriodendron* that could be used to further explore this process, we showed at both the transcriptional and metabolic levels that LtuPTOX is involved in carotenoid metabolism and orange band formation on the tepals of *L. tulipifera*, which will enable an understanding of the color formation mechanism of *L. tulipifera*.

5. Conclusions

In this study, we identified a putative LtuPTOX gene derived from *L. tulipifera* by multiple database selection. Combined with a series of transcriptional and metabolic detection, we inferred the *LtuPTOX* gene might participate in carotenoid synthesis and orange-band of the petals. In conclusion, this study will lay a foundation for further uncovering the mechanism of flower color of *L. tulipifera*.

Author Contributions: In this study, Huogen Li conceived the study, Ziyuan Hao participated in the entire experimental process as well as statistical analyses, total RNA and the full-length cDNA isolation was performed by Ziyuan Hao and Yaxian Zong, while plant culture of the tobaccos and subcellular localization study were contributed by Yaxian Zong and Ziyuan Hao, plant tissues and quantitative PCR were provided by Huanhuan Liu and Zhonghua Tu. Moreover, Ziyuan Hao completed the gene structure and protein properties analysis as well as determination of pigments content. Ziyuan Hao and Yaxian Zong drafted the manuscript and the further revision was completed by Huogen Li. Huogen Li is responsible for the manuscript as a whole.

Funding: This study was financially funded by the National Natural Science Foundation of China (31770718, 31470660) and the Priority Academic Program Development of Jiangsu Higher Education Institutions (PAPD).

Acknowledgments: The authors are appreciated about the supports from Dr. Wenjie Ding, College of Landscape Architecture, Nanjing Forestry University in tobacco transient transformation and subcellular localization assay.

Conflicts of Interest: The authors declare no conflict of interest.

Appendix A

Appendix A. Primer sequence used in the article

Promers Name	Promers Sequence	TM/℃
nG31435-F	AACCCAGGAAGACCATCTCC	57

nG31435-R	GGAGCTCTTGCTGTTTGAA	54
5GSP1	CAAATAATCAGCTCTTCTCCAC	55.6
5GSP2	CCTCCACGATAACTTCTTCCTCC	61
3GSP1	GTTTGACCGTTTTCTTGCTC	54.6
3GSP2	GGAGAAGAATTGAAAAGAATGCCTG	58.1
LtuPTOX-F	TACTCAGCAACGAATAAACC	52.2
LtuPTOX-R	TTGGATAAATATGGACCCCT	52.9
p1302-LtuPTOX-TF	actcttgaccatggtagatctATGACTACAAGATCAACATCTCTCTCTTC	60.6
p1302-LtuPTOX-TR	aagttcttctcctttactagtTTCTTGTTTCCTTTCATGAGGGG	62.4
35S primer	GACGCACAATCCCACTATCC	56
LtuPTOX-qF	CTGTTCTGCACATGTACGAGA	57.8
LtuPTOX-qR	GCAAGAAAACGGTCAAACCAC	57.9
Actin97-qF	TTCCCGTTCAGCAGTGGTCGTGGTCG	58
Actin97-qR	TGGTCGCACAACTGGTATCG	58

Appendix B

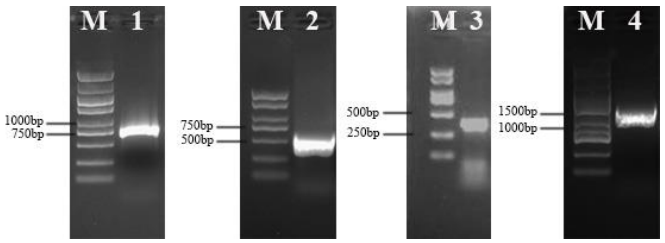

Appendix B. Isolation and detection of the LtuPTOX gene. DNA fragments were detected by 1.5% agarose gel. Lane 1 ~ 3 were the intermediate and untranslated regions of 5′ and 3′ respectively. Lane 4 was the open reading frame.

References

1. Waser, N.M.; Price, M.V. Pollinator choice and stabilizing selection for flower color in *delphinium nelsonii*. *Evolution* **1981**, *35*, 376-390.
2. Menze, R.; Shmida, A. The ecology of flower colours and the natural colour vision of insect pollinators: The israeli flora as a study case. *Biological Reviews* **1993**, *68*, 81-120.
3. Briscoe, A.D.; Chittka, L. The evolution of color vision in insects. *Annu Rev Entomol* **2001**, *46*, 471-510.
4. Vickery, R.K. Speciation in *mimulus* , or, can a simple flower color mutant lead to species divergence. *The Great Basin naturalist* **1995**, *55*, 177-180.
5. Zhang, H.F.; Wei, Q.C.; Li, C.Z.; Jiang, C.M.; Zhang, H.C. Comparative proteomic analysis provides insights into the regulation of flower bud differentiation in *crocus sativus* l. *Journal of Food Biochemistry* **2016**, *40*, 567-582.
6. Yue, Y.; Liu, J.; Shi, T.; Chen, M.; Li, Y.; Du, J.; Jiang, H.; Yang, X.; Hu, H.; Wang, L. Integrating transcriptomic and gc-ms metabolomic analysis to characterize color and aroma formation during tepal development in *lycoris longituba*. *Plants (Basel)* **2019**, *8*, 53.
7. Grotewold, E. The genetics and biochemistry of floral pigments. *Annu Rev Plant Biol* **2006**, *57*, 761-780.
8. Rodriguezconcepcion, M.; Avalos, J.; Bonet, M.L. A global perspective on carotenoids: Metabolism, biotechnology, and benefits for nutrition and health. *Progress in Lipid Research* **2018**, *70*, 62-93.

9. Carol, P.; Kuntz, M. A plastid terminal oxidase comes to light: Implications for carotenoid biosynthesis and chlororespiration. *Trends Plant Sci* **2001**, *6*, 31-36.
10. Cazzonelli, C.I.; Pogson, B.J. Source to sink: Regulation of carotenoid biosynthesis in plants. *Trends Plant Sci* **2010**, *15*, 266-274.
11. Welsch, R.; Beyer, P.; Hugueney, P.; Kleinig, H.; von Lintig, J. Regulation and activation of phytoene synthase, a key enzyme in carotenoid biosynthesis, during photomorphogenesis. *Planta* **2000**, *211*, 846-854.
12. Li, F.; Vallabhaneni, R.; Yu, J.; Rocheford, T.; Wurtzel, E.T. The maize phytoene synthase gene family: Overlapping roles for carotenogenesis in endosperm, photomorphogenesis, and thermal stress tolerance. *Plant Physiol* **2008**, *147*, 1334-1346.
13. Shahbazi, M.; Gilbert, M.; Laboure, A.M.; Kuntz, M. Dual role of the plastid terminal oxidase in tomato. *Plant Physiol* **2007**, *145*, 691-702.
14. Foudree, A.; Putarjunan, A.; Kambakam, S.; Nolan, T.; Fussell, J.; Pogorelko, G.; Rodermel, S. The mechanism of variegation in *immutans* provides insight into chloroplast biogenesis. *Frontiers in Plant Science* **2012**, *3*, 1-10.
15. Welsch, R.; Maass, D.; Voegel, T.; Dellapenna, D.; Beyer, P. Transcription factor *rap2.2* and its interacting partner *sinat2*: Stable elements in the carotenogenesis of *arabidopsis* leaves. *Plant Physiol* **2007**, *145*, 1073-1085.
16. Diner, B.; Mauzerall, D. Feedback controlling oxygen production in a cross-reaction between two photosystems in photosynthesis. *Biochimica et Biophysica Acta* **1973**, *305*, 329-352.
17. Bennoun, P. Evidence for a respiratory chain in the chloroplast. *Proc Natl Acad Sci U S A* **1982**, *79*, 4352-4356.
18. Wu, D.; Wright, D.A.; Wetzel, C.M. The immutans variegation locus of *arabidopsis* defines a mitochondrial alternative oxidase homolog that functions during early chloroplast biogenesis. *The Plant Cell* **1999**, *11*, 43-55.
19. Carol, P.; Stevenson, D.; Bisanz, C.; Breitenbach, J.; Sandmann, G.; Mache, R.; Coupland, G.; Kuntz, M. Mutations in the *arabidopsis* gene *immutans* cause a variegated phenotype by inactivating a chloroplast terminal oxidase associated with phytoene desaturation. *Plant Cell* **1999**, *11*, 57-68.
20. Wetzel, C.M.; Jiang, C.; Meehan, L.J. Nuclear-organelle interactions: The immutans variegation mutant of *arabidopsis* is plastid autonomous and impaired in carotenoid biosynthesis. *The Plant Journal* **1994**, *6*, 161-175.
21. Sun, X.; Wen, T. Physiological roles of plastid terminal oxidase in plant stress responses. *Journal of Biosciences* **2011**, *36*, 951-956.
22. Cheng, Y.; Li, H. Interspecies evolutionary divergence in liriodendron, evidence from the nucleotide variations of *lcdhn-like* gene. *BMC Evol Biol* **2018**, *18*, 195.
23. Chen, J.; Hao, Z.; Guang, X. *Liriodendron* genome sheds light on angiosperm phylogeny and species-pair differentiation. *Nature plants* **2019**, *5*, 18-25.
24. Zhou, Y.; Li, M.; Zhao, F.; Zha, H.; Yang, L.; Lu, Y.; Wang, G.; Shi, J.; Chen, J. Floral nectary morphology and proteomic analysis of nectar of *liriodendron tulipifera* linn. *Front Plant Sci* **2016**, *7*, 826.
25. Demuth, P.; Join, F.S. Carotenoid flower pigments in *liodendron* and *magnolia*. *Bulletin of the Torrey Botanical Club* **1978**, *105*, 65.
26. Liang, H.Y.; Carlson, J.E.; Leebens-Mack, J.H.; Wall, P.K.; Mueller, L.A.; Buzgo, M.; Landherr, L.L.; Hu, Y.; DiLoreto, D.S.; Ilut, D.C., *et al.* An est database for liriodendron tulipifera l. Floral buds: The first est

resource for functional and comparative genomics in *liriodendron*. *Tree Genetics & Genomes* **2008**, *4*, 419-433.

27. Roy, A.; Kucukural, A.; Zhang, Y. I-tasser: A unified platform for automated protein structure and function prediction. *Nat Protoc* **2010**, *5*, 725-738.
28. Hu, B.; Jin, J.; Guo, A.Y.; Zhang, H.; Luo, J.; Gao, G. Gsds 2.0: An upgraded gene feature visualization server. *Bioinformatics* **2015**, *31*, 1296-1297.
29. Robert, X.; Gouet, P. Deciphering key features in protein structures with the new endscript server. *Nucleic Acids Res* **2014**, *42*, W320-324.
30. Katoh, K.; Misawa, K.; Kuma, K.; Miyata, T. Mafft: A novel method for rapid multiple sequence alignment based on fast fourier transform. *Nucleic Acids Res* **2002**, *30*, 3059-3066.
31. Katoh, K.; Rozewicki, J.; Yamada, K.D. Mafft online service: Multiple sequence alignment, interactive sequence choice and visualization. *Brief Bioinform* **2017**, 1-7.
32. Dereeper, A.; Guignon, V.; Blanc, G.; Audic, S.; Buffet, S.; Chevenet, F.; Dufayard, J.F.; Guindon, S.; Lefort, V.; Lescot, M., *et al.* Phylogeny.Fr: Robust phylogenetic analysis for the non-specialist. *Nucleic Acids Res* **2008**, *36*, W465-469.
33. Arnon, D.I. Copper enzymes in isolated chloroplasts. Polyphenoloxidase in beta vulgaris. *Plant Physiol* **1949**, *24*, 1-15.
34. Kwak, M.J.; Je, S.M.; Cheng, H.C.; Seo, S.M.; Park, J.H.; Baek, S.G.; Khaine, I.; Lee, T.; Jang, J.; Li, Y., *et al.* Night light-adaptation strategies for photosynthetic apparatus in yellow-poplar (*liriodendron tulipifera* l.) exposed to artificial night lighting. *Forests* **2018**, *9*, 74.
35. Suzuki, T.; Hashimoto, T.; Yabu, Y.; Majiwa, P.A.; Ohshima, S.; Suzuki, M.; Lu, S.; Hato, M.; Kido, Y.; Sakamoto, K., *et al.* Alternative oxidase (aox) genes of african trypanosomes: Phylogeny and evolution of aox and plastid terminal oxidase families. *J Eukaryot Microbiol* **2005**, *52*, 374-381.
36. Baena-Gonzalez, E.; Allahverdiyeva, Y.; Svab, Z.; Maliga, P.; Josse, E.M.; Kuntz, M.; Maenpaa, P.; Aro, E.M. Deletion of the tobacco plastid *psba* gene triggers an upregulation of the thylakoid-associated nad(p)h dehydrogenase complex and the plastid terminal oxidase (ptox). *Plant J* **2003**, *35*, 704-716.
37. Houille-Vernes, L.; Rappaport, F.; Wollman, F.A.; Alric, J.; Johnson, X. Plastid terminal oxidase 2 (ptox2) is the major oxidase involved in chlororespiration in *chlamydomonas*. *Proc Natl Acad Sci U S A* **2011**, *108*, 20820-20825.
38. Ahmad, N.; Michoux, F.; Nixon, P.J. Investigating the production of foreign membrane proteins in tobacco chloroplasts: Expression of an algal plastid terminal oxidase. *PLoS One* **2012**, *7*, e41722.
39. Josse, E.M.; Simkin, A.J.; Gaffe, J.; Laboure, A.M.; Kuntz, M.; Carol, P. A plastid terminal oxidase associated with carotenoid desaturation during chromoplast differentiation. *Plant Physiol* **2000**, *123*, 1427-1436.
40. Wang, J.; Sommerfeld, M.; Hu, Q. Occurrence and environmental stress responses of two plastid terminal oxidases in *haematococcus pluvialis* (chlorophyceae). *Planta* **2009**, *230*, 191-203.
41. Laureau, C.; De Paepe, R.; Latouche, G.; Moreno-Chacon, M.; Finazzi, G.; Kuntz, M.; Cornic, G.; Streb, P. Plastid terminal oxidase (ptox) has the potential to act as a safety valve for excess excitation energy in the alpine plant species *ranunculus glacialis* l. *Plant Cell Environ* **2013**, *36*, 1296-1310.
42. Giuliano, G.; Bartley, G.E.; Scolnik, P.A. Regulation of carotenoid biosynthesis during tomato development. *Plant Cell* **1993**, *5*, 379-387.
43. Finnegan, P.M.; Umbach, A.L.; Wilce, J.A. Prokaryotic origins for the mitochondrial alternative oxidase and plastid terminal oxidase nuclear genes. *FEBS Lett* **2003**, *555*, 425-430.

44. McDonald, A.E.; Vanlerberghe, G.C. Origins, evolutionary history, and taxonomic distribution of alternative oxidase and plastoquinol terminal oxidase. *Comp Biochem Physiol Part D Genomics Proteomics* **2006**, *1*, 357-364.
45. Nakamura, K.; Sakamoto, K.; Kido, Y.; Fujimoto, Y.; Suzuki, T.; Suzuki, M.; Yabu, Y.; Ohta, N.; Tsuda, A.; Onuma, M., *et al.* Mutational analysis of the trypanosoma vivax alternative oxidase: The e(x)6y motif is conserved in both mitochondrial alternative oxidase and plastid terminal oxidase and is indispensable for enzyme activity. *Biochem Biophys Res Commun* **2005**, *334*, 593-600.
46. Fu, A.; Liu, H.; Yu, F.; Kambakam, S.; Luan, S.; Rodermel, S. Alternative oxidases (aox1a and aox2) can functionally substitute for plastid terminal oxidase in *arabidopsis* chloroplasts. *Plant Cell* **2012**, *24*, 1579-1595.
47. Kuntz, M. Plastid terminal oxidase and its biological significance. *Planta* **2004**, *218*, 896-899.
48. Cournac, L.; Redding, K.; Ravenel, J. Electron flow between photosystem ii and oxygen in chloroplasts of photosystem ideficient algae is mediated by a quinol oxidase involved in chlororespiration. *Journal of Biological Chemistry* **2000**, *275*, 17256-17262.
49. Sun, X.; Yang, C.Q.; Wen, T.; Zeng, F.C.; Wang, Q.; Yang, W.Y.; Lin, H.H. Water stress enhances expression of genes encoding plastid terminal oxidase and key components of chlororespiration and alternative respiration in soybean seedlings. *Z Naturforsch C* **2014**, *69*, 300-308.
50. Qian Yuqi; Wang Danfeng; Aigen, F. Molecular features and physiological roles of plant plastid terminal oxidase. *Plant Physiology Journal* **2016**, *52*, 1710-1720.
51. Kambakam, S.; Bhattacharjee, U.; Petrich, J.; Rodermel, S. Ptox mediates novel pathways of electron transport in etioplasts of *arabidopsis*. *Mol Plant* **2016**, *9*, 1240-1259.